
In vitro* and *in vivo* photodynamic efficacies of novel and conventional phenothiazinium photosensitizers against multidrug-resistant *Candida auris

Patrícia Helena Grizante Barião^{1†}, Ludmilla Tonani^{1†}, Guilherme Thomaz Pereira Brancini¹, Erika Nascimento², Gilberto Úbida Leite Braga¹, Mark Wainwright³, and Marcia Regina von Zeska Kress^{1,*}

¹ Departamento de Análises Clínicas, Toxicológicas e Bromatológicas, Faculdade de Ciências Farmacêuticas de Ribeirão Preto, Universidade de São Paulo, Ribeirão Preto, SP 14040-903, Brazil; P.H.G.B., patriciahelena92@hotmail.com (ORCID 0000-0003-1335-3975); L.T., ludmilla@fcrp.usp.br (ORCID 0000-0001-6892-8962); G.T.P.B., guilherme.brancini@usp.br (ORCID 0000-0001-9726-6056); G.U.L.B., gbraga@fcrp.usp.br (ORCID 0000-0002-4787-4704)

² Departamento de Clínica Médica, Faculdade de Medicina de Ribeirão Preto, Universidade de São Paulo, Ribeirão Preto, SP, 14048-900, Brazil; E.N., erika.nascimento@gmail.com (ORCID 0000-0002-4141-7414)

³ School of Pharmacy and Biomolecular Sciences, Liverpool John Moores University, Liverpool L3 3AF, United Kingdom; M.W., mark_wainwright@hotmail.com (ORCID 0000-0002-4736-7462)

* Correspondence: Marcia Regina von Zeska Kress, Av. do Cafe, s/n Ribeirão Preto, São Paulo, Brazil 14040-903. kress@fcrp.usp.br (ORCID 0000-0003-1239-7722)

† These authors contributed equally to this work.

Abstract: The fast-emerging and multidrug-resistant *Candida auris* is the first fungal pathogen to be considered a threat to global public health. Thus, there is a high unmet medical need to develop new therapeutic strategies to control this species. Antimicrobial photodynamic therapy (APDT) is a promising alternative that simultaneously targets and damages numerous microbial biomolecules. Here, we investigated the *in vitro* and *in vivo* effects of APDT with four phenothiazinium photosensitizers: (i) methylene blue (MB), (ii) toluidine blue (TBO), and two MB derivatives, (iii) new methylene blue (NMBN) and (iv) the pentacyclic derivative S137, against *C. auris*. To measure the *in vitro* efficacy of each PS, minimal inhibitory concentrations (MICs) and survival fraction were determined. Also, the efficiency of APDT was evaluated *in vivo* with the *Galleria mellonella* insect model for infection and treatment. Although the *C. auris* strain used in our study was shown to be resistant to the most-commonly used clinical antifungals, it could not withstand the damages imposed by APDT with any of the four photosensitizers. However, for the *in vivo* model, only APDT performed with S137 allowed survival of infected *G. mellonella* larvae. Our results show that structural and chemical properties of the photosensitizers play a major role on the outcomes of *in vivo* APDT and underscore the need to synthesize and develop novel photosensitizing molecules against multidrug-resistant microorganisms.

Keywords: antimicrobial photodynamic therapy; *Candida auris*; *Galleria mellonella*; multidrug-resistance; phenothiazinium photosensitizers.

1. Introduction

Candida species play a major role in nosocomial fungal infections worldwide, being the fourth most common causative agent. The most frequent species recovered from human infection is *C. albicans*, followed by non-*albicans* species such as *C. parapsilosis*, *C. tropicalis*, *C. glabrata*, and *C. krusei*. Owing to their high resistance to antifungal agents, all species present worrying therapeutic failure rates [1].

Candida auris, which is a member of the *C. haemulonii* complex, is a fast emerging multidrug-resistant fungus. Since 2009, when it was first reported, it has been isolated and present on five continents [2]. Human skin is considered the primary site of colonization by this fungus which, unlike *C. albicans*, is rarely isolated from the genitourinary and gastrointestinal tracts. This new species is capable of causing invasive infections and is generally hospital-acquired [3]. *Candida auris* is the first fungal pathogen to be considered a threat to global public health. This fungus contaminates hospital settings for a prolonged time, including surfaces, equipment, and fomites. Thus, a contaminated patient room can easily lead to *C. auris* transmission to patients and hospital workers alike, causing colonization and/or infection [4].

C. auris is able to form biofilms on both abiotic and biotic surfaces, e.g., human tissue and implanted medical devices, and this ability is associated with its colonization persistence [5]. Enhanced biofilm growth by *C. auris* was observed on a skin *ex vivo* model [6], and this structure was shown to survive on fomites for up to two weeks [7]. Biofilms play a role not only in persistence in healthcare settings, but also in drug resistance [8].

The main concern regarding *C. auris* is its resistance to many classes of clinical antifungal drugs, which may be one deciding factor for its high mortality rates [9]. Specifically, *C. auris* is, on many instances, resistant to azoles, polyenes, and echinocandins [2]. Strains of *C. auris* are frequently resistant to fluconazole and are commonly resistant to amphotericin B, voriconazole, and caspofungin [10]. The occurrence of multidrug-resistant strains of *C. auris* constitutes a significant issue as it virtually eliminates the most widely used therapeutic approaches and represents a major threat to both patients and healthcare workers.

Given the multidrug resistance of *C. auris* clinical isolates to commercial antifungals, the development of new therapeutic strategies is currently necessary. Antimicrobial photodynamic therapy (APDT) is an innovative technology that, contrary to conventional antimicrobial drugs, does not have specific molecular targets and, consequently, simultaneously damages numerous biomolecules. This unspecific mode-of-action makes the development of resistance unlikely and also bypasses known resistance mechanisms [11]. Therefore, APDT could be a clinically useful therapeutic strategy against many multidrug resistant pathogens, including *C. auris* [12].

Mechanistically, APDT achieves extensive cellular damage by combining three factors, namely, visible light, molecular oxygen, and a photosensitizer (PS). The latter molecule is responsible for absorbing light and transferring either energy or electrons to molecular oxygen, resulting in the production of reactive oxygen species (ROS), which, in turn, oxidize a diversity of biomolecules and kill the pathogen [13]. Phenothiazinium PSs, such as methylene blue (MB) and toluidine blue (TBO), are among the most used PSs in APDT as they present low toxicity and are clinically approved for human use [14-16]. Photosensitizers with different structures vary in many properties, such as cell attachment efficiency and localization, both of which greatly influence the efficacy of APDT [17, 18]. As such, PSs may be chemically modified to produce novel molecules with improved properties. For instance, derivatives such as new methylene blue N (NMBN) and the pentacyclic PS S137 were developed from and shown to be more effective than MB [18-20]. APDT with phenothiazinium PSs has been used to kill a diversity of both yeasts and filamentous fungi, including *Candida* [21-24], *Metarhizium*, *Aspergillus* [25], *Fusarium* [26, 27], *Colletotrichum* [28-30], *Neoscytalidium* [31], *Scedosporium* and *Lomentospora* [32], *Exophiala* [33], and *Rhizopus* [34].

The virulence of *Candida* species is usually evaluated by the gold standard murine model [35]. However, insect models such as those using larvae of *Galleria mellonella* (greater wax moth) have been successfully used to study *C. albicans* infections [36, 37] and treatments [38, 39]. The insect model reproduces most aspects of mammalian infection, can survive at 37 °C, allows the inexpensive obtainment of large numbers of larvae, and its use requires no approval by ethics committees [37].

Here we evaluated the *in vitro* and *in vivo* effects of APDT with the phenothiazinium PSs MB, TBO, NMBN, and S137 against *C. auris*, using the *G. mellonella* insect infection and treatment model.

2. Material and Methods

2.1. Strains and growth conditions

The CDC B11903 strain of *C. auris* was obtained from Microbiologics (St. Cloud, MN, USA). Also, *C. albicans* strain ATCC 64548 and *C. parapsilosis* strain ATCC 22019 were obtained from the American Type Culture Collection (ATCC). Blastospores were inoculated on Sabouraud dextrose agar (SDA) culture media (KASVI, Spain) and incubated in the dark at 35 °C for two days. Freshly grown blastospores were used to inoculate 20 mL of yeast peptone dextrose (YPD) medium, which was then incubated in an orbital shaker at 35 °C until stationary growth. Cells were harvested and washed in sterile phosphate-buffered saline (PBS) (10 mM phosphate buffer [J. T. Baker, Mexico], 2.7 mM potassium chloride [J. T. Baker, Mexico], 137 mM sodium chloride [Fluka®, Germany], pH 7.4). Blastospore concentration was adjusted with PBS by counting in a hemacytometer.

2.2. *In vitro* antifungal susceptibility testing

Susceptibility testing was conducted according to the broth dilution method (M27-A3) from the Clinical and Laboratory Standards Institute (CLSI) [40]. The antifungal drugs amphotericin B (AMB), voriconazole (VOR), and posaconazole (POS) were purchased from Sigma Aldrich (St. Louis, USA). Itraconazole (ITR) was purchased from Fragon (India). Concentrations ranged from 0.03 to 16 $\mu\text{g mL}^{-1}$. The experiments were performed in 96-well, flat-bottomed plates with RPMI 1614 culture medium (Gibco, Invitrogen) buffered with 0.165 M 3-(N-morpholino)propanesulfonic acid (MOPS [J. T. Baker, Mexico]), pH 7.0, antifungal drugs, and 2.5×10^3 cells mL^{-1} of *C. auris*, *C. albicans*, and *C. parapsilosis*. After 48 h of incubation at 35 °C, the MIC was determined spectrophotometrically at 492 nm using a microplate reader (Epoch – Biotek). The MIC was considered the lowest concentration that inhibits fungal growth by 100% for AMB and by $\geq 80\%$ for ITR, VOR, and POS.

The minimal fungicidal concentration (MFC) was evaluated by the dropout method. An aliquot of 10 μL obtained from each well of the *in vitro* antifungal susceptibility testing that showed no visible growth was inoculated on SDA plates (35 °C for 48 h). The MFC was considered as the lowest antifungal concentration killing 100% of the inoculum.

2.3. Aggregates and biofilm

The evaluation of the aggregate-forming phenotype of *C. auris* blastoconidia was performed by optical microscopy of a 4×10^8 cells mL^{-1} suspension at 400x magnification (N120, Coleman). Images were registered with the HDCE-X5 camera with the ScopImage 9.0 software.

The conditions for biofilm formation were optimized according to Pierce et al. [41]. Briefly, blastoconidia were suspended in RPMI 1640 supplemented with L-glutamine, buffered with MOPS (J. T. Baker, USA) and adjusted to 1.0×10^6 cells mL^{-1} by counting in a hemocytometer. Biofilms were formed by inoculating 100 μL of cell suspensions into wells of 96-well plates and incubating at 35 °C for 18 h. After biofilm formation, growth medium was removed and nonadherent cells were washed out with sterile PBS. To measure biofilm biomass and extracellular matrix, the adhered biofilm was fixed with 200 μL of 100% methanol for 15 minutes. Total biofilm biomass was measured according to Li et al. [42]. Briefly, 200 μL of a 0.5% (w/v) crystal violet solution (SIGMA, USA) was added to the biofilm, followed by incubation for 20 min. The excess stain was gently removed and any residue was washed out with PBS. The biofilm was then destained by adding 200 μL of 33% acetic acid for 5 min. Biomass density was determined spectrophotometrically by measuring the destaining solution at 570 nm on a microplate reader (Epoch – Biotek). Extracellular matrix was measured according to Seidler et al. [43]. Briefly, 200 μL of 1% (w/v) safranin (SIGMA, USA) was added to the biofilm, followed by incubation for 5 min. The excess stain was gently removed and any residue was washed out with PBS. The biofilm was then destained by adding 200 μL of 33% acetic acid for 5 min. Extracellular matrix density was determined spectrophotometrically by measuring the destaining solution at 492 nm on a microplate

reader (Epoch – Biotek). The biofilm biomass and extracellular matrix absorbance results were used to create a correlation plot with the GraphPad Prism 5 software (GraphPad Software, San Diego, California, USA).

2.4. Photosensitizers and light source

The phenothiazinium PS methylene blue (MB), new methylene blue N (NMBN), and toluidine blue O (TBO) were purchased from Sigma Aldrich (USA). The novel pentacyclic phenothiazinium PS S137 (DO15) was synthesized as previously described [20]. Stock solutions of all PS were prepared with PBS and stored at -20°C . Light exposure was carried out with an array of 96 light-emitting diodes (emission peak = 635 nm; irradiance = 15.23 mW cm^{-2}) and APDT experiments were performed with a light fluence of 15 J cm^{-2} (16.37 min exposure).

2.5. Evaluation of APDT based on PS MIC

The best conditions for APDT against *C. auris* were determined by conducting MIC-based experiments [22, 28, 31]. Fifty microliters of a blastoconidia suspension ($5 \times 10^3\text{ cells mL}^{-1}$) and 50 μL of a PS solution were added to each well of a 96-well plate. Final concentrations of MB were 0.5, 0.9, 1.9, 3.8, 7.5, 15, and 29.9 $\mu\text{g mL}^{-1}$; NMBN were 0.5, 1, 2.1, 4.2, 8.3, 16.6, and 33.3 $\mu\text{g mL}^{-1}$; TBO were 0.4, 0.8, 1.5, 3.1, 6.1, 12.2, and 24.4 $\mu\text{g mL}^{-1}$; and S137 were 0.6, 1.1, 2.2, 4.5, 9.0, 17.9 and 35.9 $\mu\text{g mL}^{-1}$. Plates were incubated in the dark for 30 min at room temperature and were either exposed to light or kept in the dark (dark control). Then, 100 μL of 2 \times concentrated RPMI 1614 buffered with 0.165 M MOPS pH7.0 were added to each well and plates were incubated at 35°C in the dark. Fungal growth in each well was visually assessed after four days. MICs were defined as the lowest concentration resulting in total growth inhibition. Two independent experiments in triplicates were performed.

2.6. Effect of APDT on blastoconidia survival

Based on the obtained MIC values and according to Rodrigues et al. [22], the effects of APDT on the survival of blastoconidia was determined. Fifty microliters of a blastoconidia suspension and 50 μL of a PS solution (MB, NMBN, TBO, or S137) were added to each well of a 96-well plate. The final concentration of blastoconidia in the mixture was $1 \times 10^7\text{ cells mL}^{-1}$, and the final concentration of MB, NMBN, TBO, and S137 were 7.5, 2.1, 6.1, and 2.2 $\mu\text{g mL}^{-1}$, respectively. Plates were pre-incubated in the dark for 30 min at room temperature and then either exposed to light or kept in the dark (dark control). Then, blastoconidia suspensions were collected, serially diluted 10-fold in PBS, and 50 μL of each dilution was spread onto SDA (KASVI, Spain) supplemented with 0.12 g L^{-1} deoxycholic acid sodium salt (Fluka, Italy). Plates were incubated in the dark at 35°C for 24 h. Colony-forming units (CFU) were counted under a stereomicroscope (8 \times magnification, SZX7, Olympus) for up to 4 days. Controls with blastoconidia exposed to light (15 J cm^{-2}) in the absence of PS and treated with PS but

not exposed to light were prepared in parallel for all treatments. The effect of different concentrations of PSs was estimated by the survival fraction, which was calculated by dividing the CFU count of treated samples by the CFU count of control samples (not exposed to either PS or light). After four days, blastoconidia that did not form colonies were considered fully inactivated by the treatment. Two independent experiments in triplicates were performed.

2.7. Virulence of *C. auris* and *C. albicans* towards *G. mellonella*

The virulence of *C. auris* and *C. albicans* were evaluated in *G. mellonella* according to Paziani et al. [27] with modifications. Groups of ten *G. mellonella* larvae at the sixth instar (weighing 225 ± 25 mg) and not presenting cuticle pigmentation were selected and placed in Petri dishes. For inoculum preparation, blastoconidia from YPD-24 h culture was harvested and washed in PBS. Cell density was adjusted with PBS by counting in a hemocytometer. Five microliters of blastoconidia were injected in the last left proleg of each larva with a 10 μ L Hamilton syringe (Hamilton, 80330 – 701RN, USA). Final concentrations of 5×10^5 , 1×10^6 , and 2×10^6 cells/larva were assayed to monitor the virulence of *C. auris* and *C. albicans*. In all trials, two uninfected groups were used as controls: (1) untouched (*naïve*) larvae and (2) larvae injected with 5 μ l PBS. The larvae were maintained in the dark at 35 °C. Survival counts of live and dead larvae were determined by visual inspection of movement and melanization every 24 h for up to eight days post-infection.

2.8. APDT in vivo assay with *G. mellonella* infected with *C. auris* or *C. albicans*

The effects of APDT on larva survival were evaluated in groups of ten *G. mellonella* larvae infected with *C. auris* or *C. albicans*. The final blastoconidia concentration injected in each larva was 1×10^6 cells and the final concentrations of PSs were 3.7 and 7.5 mg kg⁻¹ for MB, 2.1 and 4.2 mg kg⁻¹ for NMBN, 3.1 and 6.1 mg kg⁻¹ for TBO, and 4.5 and 9.0 mg kg⁻¹ for S137. For injection, a 5 μ l inoculum was prepared containing both a blastoconidia suspension and a PS solution. After injection in the last left proleg, larvae were pre-incubated in the dark for 30 min at room temperature and either exposed to light or kept in the dark (dark control). Two uninfected groups were used as controls: (1) untouched (*naïve*) larvae and (2) larvae injected with 5 μ l PBS. The larvae were kept in the dark at 35 °C. Survival counts of live and dead insects were determined by observing movement and melanization every 24 h for up to eight days post-infection. Three experiments were performed.

2.9. Statistics

All instances of statistical testing were performed with Prism 5 software (GraphPad Software, La Jolla, CA, USA). The biofilm and APDT data were assessed via one-way analysis of variance (ANOVA) with Tukey's post-hoc test. Statistical significance was set to 0.05. For the *in vivo* model, statistical analyses were carried out with a logrank (or Mantel-Cox) test. Statistical significance was set to 0.05.

3. Results

3.1. Susceptibility to antifungals

To investigate the resistance of *C. auris* to antifungals, we established the *in vitro* MIC of AMB, ITR, VOR, and POS. The antifungal MIC values for *C. albicans* and *C. parapsilosis* were used as controls. In our study, *C. auris* exhibited high MIC values for AMB, ITR, VOR, and POS (Table 1). A different pattern was observed for *C. albicans* and *C. parapsilosis*, which displayed susceptibility to the antifungal agents (Table 1).

To further investigate antifungal susceptibility, endpoint plating of a selection of the strains from the MIC assays was performed to establish minimum fungicidal concentrations (MFCs). The antifungals tested were fungicidal to *C. albicans* and *C. parapsilosis*, whereas none of the antifungals exhibited fungicidal activity against *C. auris* (Table 1). Thus, *C. albicans* and *C. parapsilosis* were susceptible to antifungals while *C. auris* presented a profile consistent with multidrug-resistance.

Table 1. Minimal inhibitory concentration (MIC) and minimal fungicidal concentration (MFC) ($\mu\text{g ml}^{-1}$) of antifungals against *C. auris*, *C. albicans*, and *C. parapsilosis*.

Strains	$(\mu\text{g mL}^{-1})$							
	AMB		ITR		VOR		POS	
	MIC	MFC	MIC	MFC	MIC	MFC	MIC	MFC
<i>C. auris</i> (CDC B11903)	2	2	>16	>16	>16	>16	>16	>16
<i>C. albicans</i> (ATCC 64548)	0.50	0.50	0.25	0.25	0.03	0.03	0.25	0.25
<i>C. parapsilosis</i> (ATCC 22019)	1	1	0.12	0.50	0.06	0.06	0.25	0.25

AMB, amphotericin B; ITR, itraconazole; VOR, voriconazole; POS, posaconazole; MIC, minimal inhibitory concentration; MFC, minimal fungicidal concentration.

3.2. Aggregates and biofilm formation

The aggregate-forming ability of *C. auris* was investigated by microscopic inspection. Aggregates-forming and non-aggregates-forming features were observed to *C. auris* and *C. albicans*, respectively (Figure 1). Thus, we show that the *C. auris* strain used in this study always presents the aggregates-forming phenotype, and it influences the pathogenicity of the fungus [36].

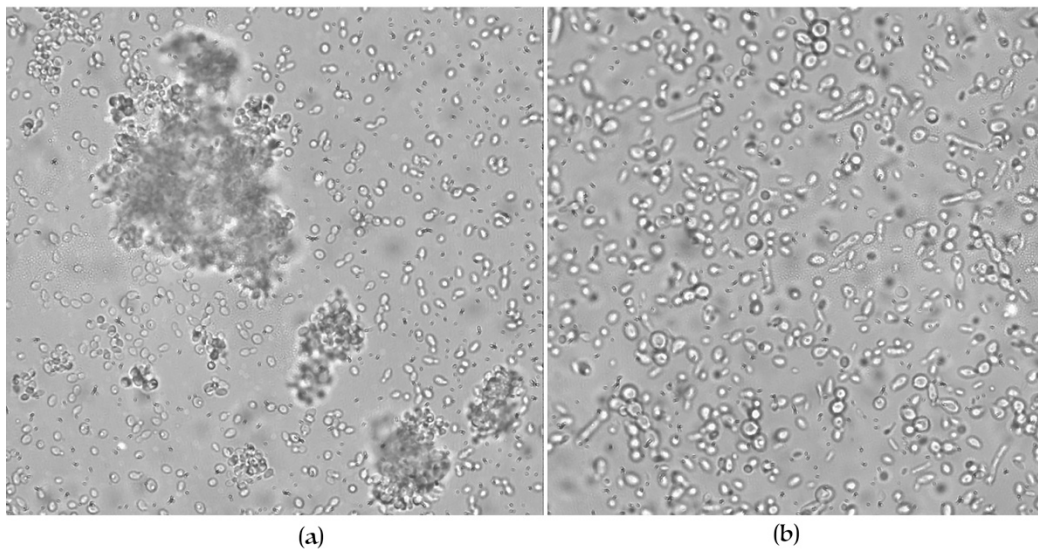


Figure 1. Microscopy images of (a) *C. auris* (aggregate-forming) and (b) *C. albicans* (non-aggregate-forming) in PBS. Blastocystidia suspensions were subjected to microscopical examination at 400× magnification.

We investigated the ability of *C. auris* to form biofilm by measuring biofilm biomass and extracellular matrix. Biofilms of *C. auris* had a higher biomass and extracellular matrix content than *C. albicans* and *C. parapsilosis* (Table 2).

Table 2. Biofilm (biomass and extracellular matrix) of *C. auris*, *C. albicans*, and *C. parapsilosis*.

Strains	Biomass (570 nm)	Matrix (492 nm)
<i>C. auris</i> (CDC B11903)	0.294	0.129
<i>C. albicans</i> (ATCC 64548)	0.073	0.010
<i>C. parapsilosis</i> (ATCC 22019)	0.021	0.000

A correlation plot was designed to show better the relation between biofilm biomass and extracellular matrix absorbance values. The results indicate that the higher the biomass value, the higher the extracellular matrix value (Figure 2). It is also shown that *C. auris* produces more biofilm biomass and extracellular matrix than *C. albicans* and *C. parapsilosis* (one-way ANOVA followed by Tukey's post-test, $P < 0.05$).

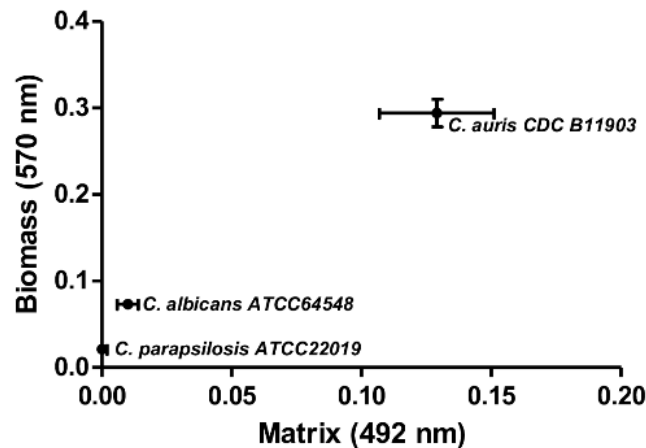


Figure 2. Correlation plot of biofilm biomass and extracellular matrix of *C. auris*, *C. albicans*, and *C. parapsilosis*.

3.3. In vitro APDT based on PS MIC and survival fraction

Given the multidrug resistant profile of *C. auris*, here we investigated the efficacy of APDT with phenothiazinium PSs. First, the APDT MIC was evaluated to determine the best conditions for the killing assay. Exposure to red light alone (15 J cm^{-2}) did not inhibit the growth of either *C. auris* or the control strains *C. albicans* and *C. parapsilosis*. In the absence of light exposure, treatment with MB, NMBN, TBO, and S137 in concentrations up to 29.9 , 33.3 , 24.4 , and $35.9 \mu\text{g mL}^{-1}$, respectively, did not inhibit the growth of any strain (Table 3). The MICs of each PS at 15 J cm^{-2} are shown in Table 3. Based on the values, all PSs were effective against *C. auris*, *C. albicans*, and *C. parapsilosis*.

Table 3. Minimal inhibitory concentration (MIC, $\mu\text{g mL}^{-1}$) of APDT against *C. auris*, *C. albicans*, and *C. parapsilosis*.

Strains/Fluence	$(\mu\text{g mL}^{-1})$							
	MB		NMBN		TBO		S137	
	0 J cm^{-2}	15 J cm^{-2}	0 J cm^{-2}	15 J cm^{-2}	0 J cm^{-2}	15 J cm^{-2}	0 J cm^{-2}	15 J cm^{-2}
<i>C. auris</i> (CDC B11903)	>29.9	1.9-3.8	>33.33	0.5-1.0	>24.4	0.8-3.1	>35.9	1.1
<i>C. albicans</i> (ATCC 64548)	>29.9	1.9	>33.33	0.5	>24.4	0.8	>35.9	0.6
<i>C. parapsilosis</i> (ATCC 22019)	>29.9	1.9-3.8	>33.33	0.5-1.0	>24.4	0.8-3.1	>35.9	0.6-1.1

MB, methylene blue; NMBN, new methylene blue N; TBO, toluidine blue O; S137, novel pentacyclic phenothiazinium photosensitizer; 0 J cm^{-2} , dark; 15 J cm^{-2} , red light.

Then, we used the determined MIC values to investigate the effects of APDT on the survival of *C. auris*. APDT (15 J cm^{-2}) with MB ($7.5 \mu\text{g mL}^{-1}$), NMBN ($2.1 \mu\text{g mL}^{-1}$), TBO ($6.1 \mu\text{g mL}^{-1}$), and S137 ($2.2 \mu\text{g mL}^{-1}$) resulted in 5-log, 5-log, 5-log, and 2-log reduction, respectively, in the survival of *C. auris* (Figure 3A); 5-log, 5-log, 5-log, and 5-log reduction, respectively, in the survival of *C. albicans* (Figure 3B) and *C. parapsilosis* (Figure 3 C). Photodynamic inactivation of blastoconidia of *C. auris*, *C. albicans*, and *C. parapsilosis* was observed for all PS ($P < 0.05$ for all treatment comparisons). Exposure to red light alone (15 J cm^{-2}) and treatment with MB, TBO, NMBN, or S137 in the dark did not kill blastoconidia of any species (Figures 3).

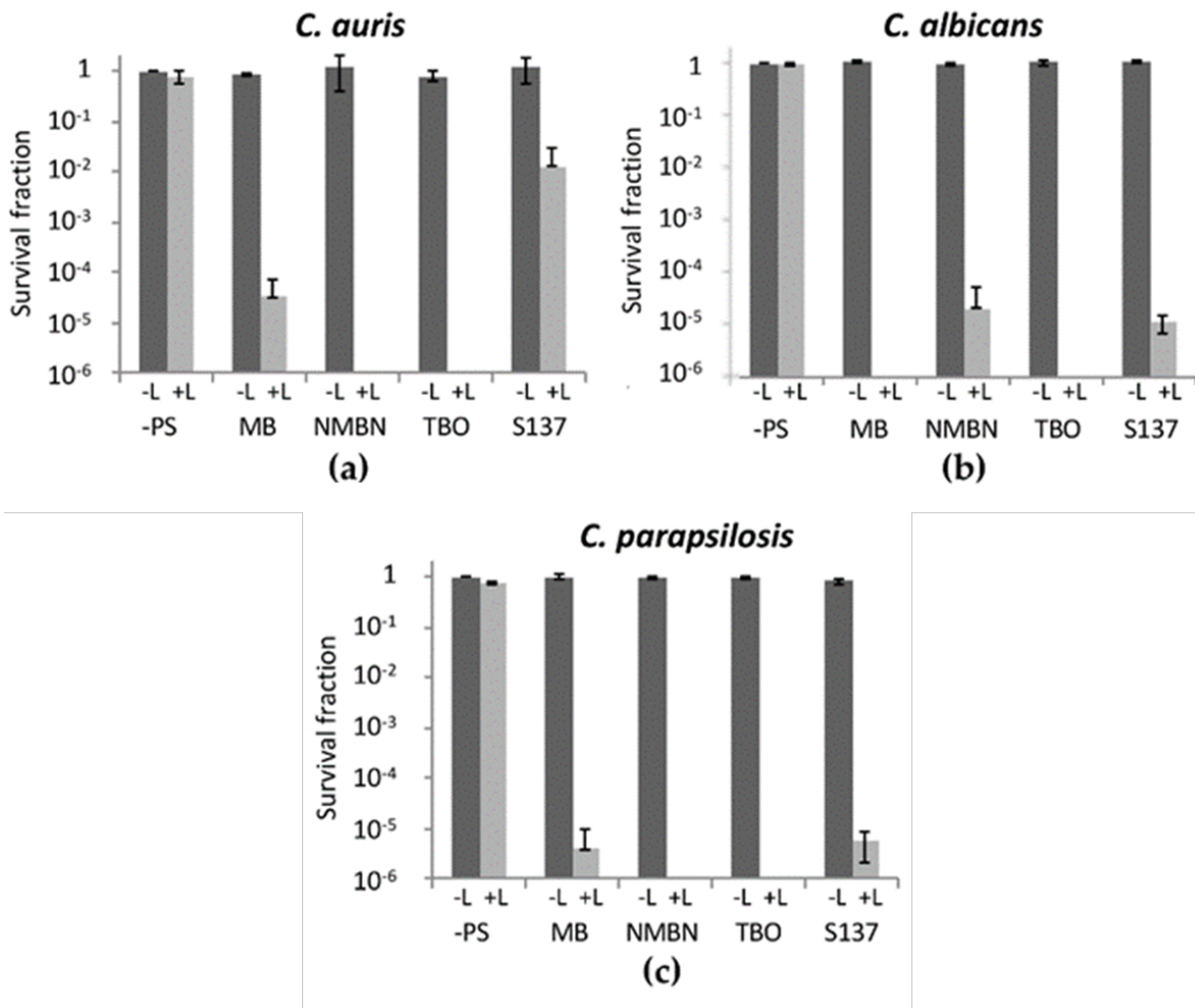


Figure 3. Photodynamic inactivation of *Candida* spp. blastoconidia. APDT of (a) *C. auris*, (b) *C. albicans*, and (c) *C. parapsilosis* with MB ($7.5 \mu\text{g mL}^{-1}$), NMBN ($2.1 \mu\text{g mL}^{-1}$), TBO ($6.1 \mu\text{g mL}^{-1}$), and S137 ($2.2 \mu\text{g mL}^{-1}$). Error bars are the standard deviation from three independent experiments. -PS, no

photosensitizer used; MB, methylene blue; NMBN, new methylene blue N; TBO, toluidine blue O; S137, novel pentacyclic phenothiazinium; -L, dark; +L, light (15 J cm^{-2}).

3.4. Virulence of *C. auris* and *C. albicans* towards *G. mellonella* larvae

Inocula of *C. auris* and *C. albicans* containing 5×10^5 , 1×10^6 , and 2×10^6 blastoconidia/larva were assayed to investigate virulence in *G. mellonella* (Figure 4). Inocula of 5×10^5 cells/larva of *C. albicans* did not reduce larval survival until eight days post-infection compared to the uninfected control (*naïve* and PBS) (Figure 4A). In contrast, inocula of 2×10^6 cells/larva killed all larvae in the second day post-infection. Therefore, the inoculum of 1×10^6 cells/larva, which kills 100% of the larvae by the 7th (*C. auris*) and third (*C. albicans*) day after microconidia injection was considered optimum for producing acute infection of *C. auris* and *C. albicans* in *G. mellonella*, respectively (Figure 4). Therefore, in the concentration used for the APDT experiments (1×10^6 cells/larva), *C. auris* was less virulent than *C. albicans* ($P < 0.0001$).

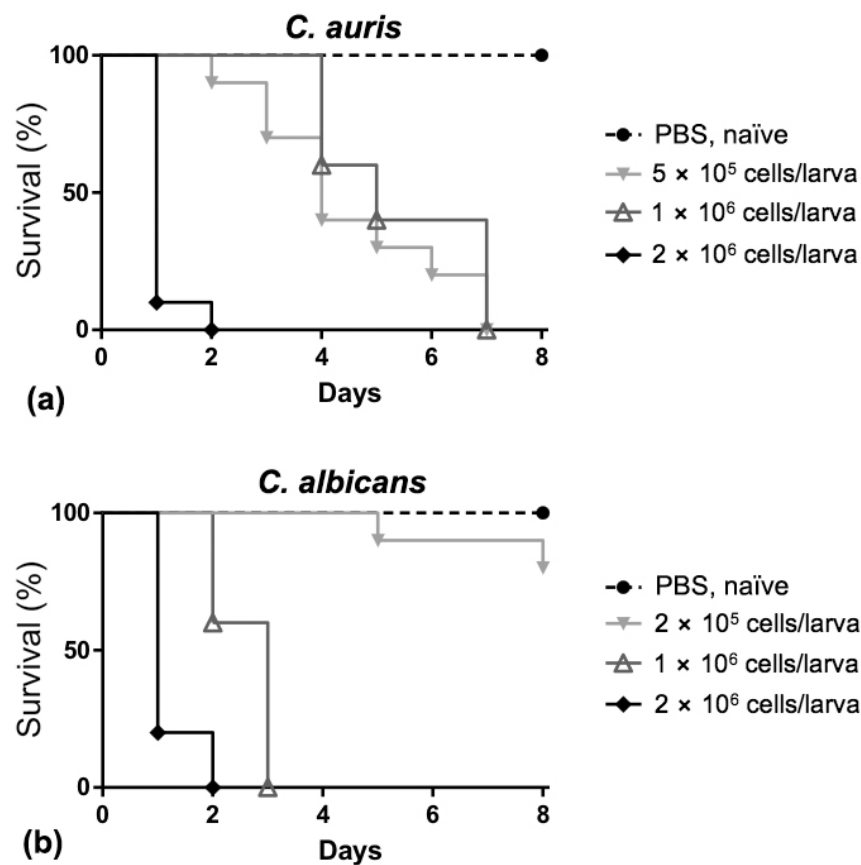


Figure 4. Virulence of (a) *C. auris* and (b) *C. albicans* in *G. mellonella* larvae. The graphs are representative of three independent experiments.

3.5. APDT in vivo assay with *G. mellonella* infected with *C. auris* or *C. albicans*

APDT with MB, NMBN, TBO, and S137 was evaluated in *G. mellonella* larvae infected with 1×10^6 cells/larva of *C. auris* and *C. albicans* (Figure 5; Supplementary Figure 1). The toxicity of the PSs MB, NMBN, and S137 in the darkness or after exposure to light (15 J cm^{-2}) was previously tested in *G. mellonella* larvae, and they were found to be non-toxic (Figure 5A-B) [27]. APDT with MB (7.5 mg kg^{-1}), NMBN (4.2 mg kg^{-1}), and TBO (6.1 mg kg^{-1}) did not prevent the killing of most larvae infected with *C. auris* and *C. albicans* (Figure 5C-H). In contrast, the injection of S137 (9 mg kg^{-1}) in *G. mellonella* infected with *C. auris* prevented the killing of 60% of the larvae (Figure 5I). This survival rate was the same for both light-exposed and non-exposed larvae. For *C. albicans*, treatment with S137 at 9 mg kg^{-1} resulted in a survival rate of 60% in the absence of light and 100% for light-exposed larvae (Figure 5J). Therefore, S137 displayed antifungal activity in *G. mellonella* infected with *C. auris* and *C. albicans*, albeit light exposure not increasing the activity for the former.

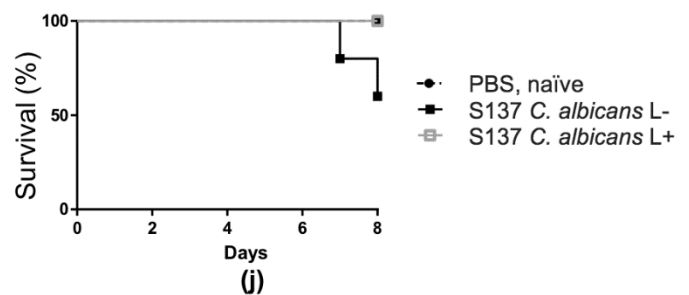
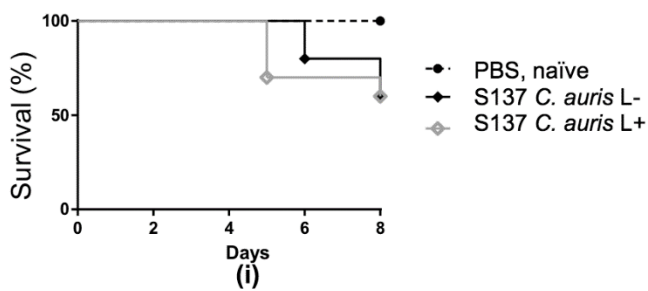
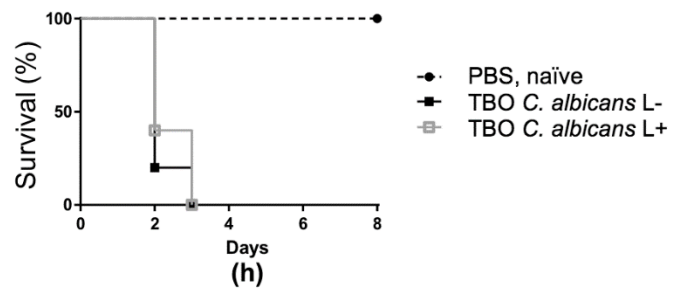
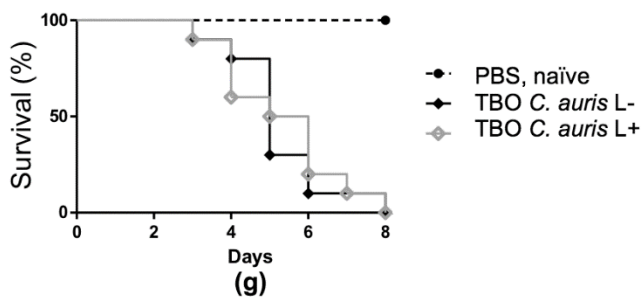
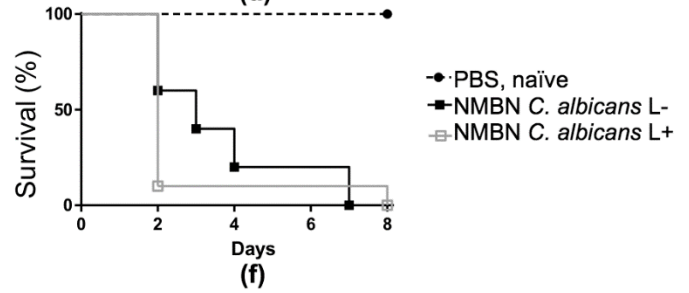
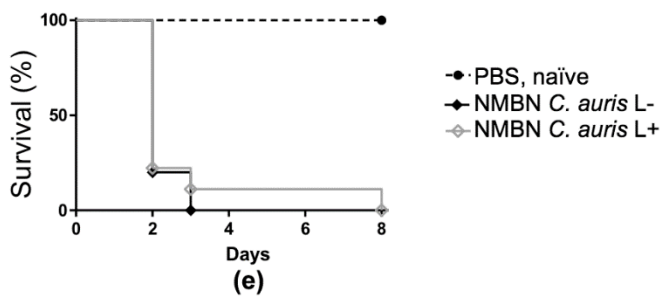
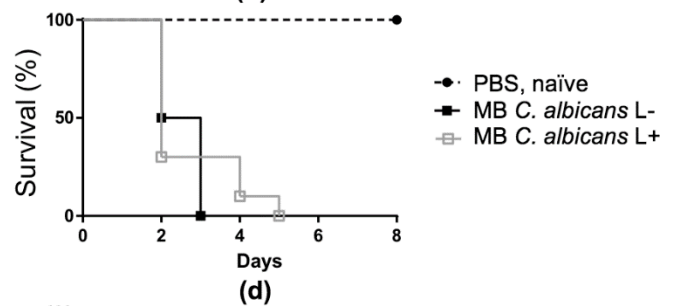
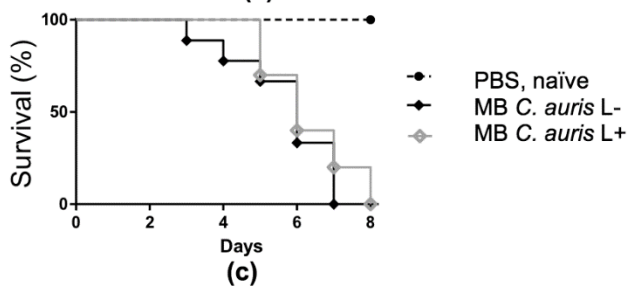
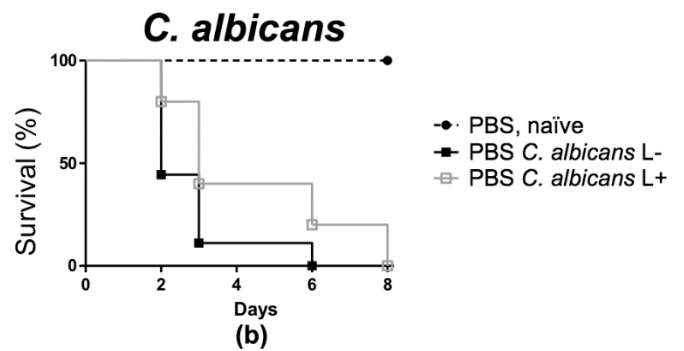
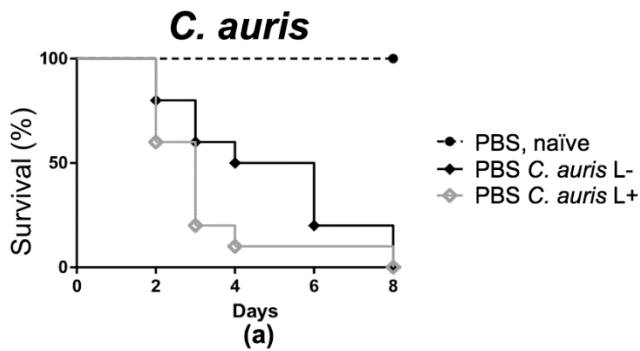


Figure 5. The *in vivo* APDT in *G. mellonella* larvae infected with *C. auris* and *C. albicans*. (a) PBS *C. auris*; (b) PBS *C. albicans*; (c) MB (7.5 mg kg⁻¹) *C. auris*; (d) MB (7.5 mg kg⁻¹) *C. albicans*; (e) NMBN (4.2 mg kg⁻¹) *C. auris*; (f) NMBN (4.2 mg kg⁻¹) *C. albicans*; (g) TBO (6.1 mg kg⁻¹) *C. auris*; (h) TBO (6.1 mg kg⁻¹) *C. albicans*; (i) S137 (9.0 mg kg⁻¹) *C. auris*; and (j) S137 (9.0 mg kg⁻¹) *C. albicans*. The graphs are Kaplan-Meier plots of *G. mellonella* survival after injection with 1×10⁶ cells/larva of the indicated *Candida* species.

4. Discussion

Candida auris is an emerging and difficult-to-detect pathogen often displaying multidrug-resistance that has been causing severe illnesses and outbreaks worldwide. Consequently, new treatment options are required to deal with this global health threat, especially for strains with multidrug-resistant profiles [2]. APDT is a promising therapeutic strategy based on photosensitizing molecules that generate ROS that kill the target pathogen upon exposure to light of suitable wavelength and fluence [13].

Here, we evaluated the efficiency of APDT with phenothiazinium PSs against *C. auris* both *in vitro* and *in vivo*. Most, but not all, *C. auris* isolates are multidrug-resistant [10]. In our *in vitro* susceptibility study, AMB, ITR, VOR, and POS presented high MICs against *C. auris*, whereas the same antifungals presented low MICs against *C. albicans* and *C. parapsilosis*. Thus, the *C. auris* strain used here presented a multidrug-resistance profile by simultaneously showing resistance to polyenes and azoles.

The multidrug-resistant phenotype underscores the necessity to test different strategies to treat *C. auris*. The use of APDT with the phenothiazinium PSs MB, NMBN, TBO, and S137 showed *in vitro* activity against planktonic *C. auris*, *C. albicans*, and *C. parapsilosis*. Similarly, a previous study showed that *C. albicans* and *C. parapsilosis* are susceptible to APDT with the phenothiazinium PSs MB, NMBN, TBO, and S137 [27]. Additionally, photodynamic treatment with NMBN (400 μM), TBO (400 μM), or MB (25-100 μM) plus red light exposure was effective against biofilms of both *C. auris* and *C. albicans* [12, 23, 24].

Aiming at potential future uses of this technique in humans, *in vivo* assays were performed. To do this, effective animal models are needed. In general, invertebrate animal infection models, such as those employing insects, provide a fast and inexpensive method to study pathogenesis and treatment options. In this sense, *G. mellonella* larvae have been used to evaluate *C. auris* pathogenesis and the effects of antifungal therapies on treating *C. auris* infections [8]. First, we evaluated the virulence of *C. auris* and *C. albicans* towards *G. mellonella*. Although *C. auris* was more effective at forming biofilms, it was less virulent than *C. albicans*. This lower virulence of *C. auris* was previously observed in murine and invertebrate infections models [35, 36]. A possible reason for the decreased virulence of *C. auris*

relative to *C. albicans* is that the former is unable to develop hyphae or pseudohyphae inside the host, an important morphological feature of *Candida* species that contributes to tissue invasion during infection [45, 46]. An additional feature that influences the pathogenicity of *C. auris* is its strain-specific ability to form (or not form) aggregates [36, 47]. The *C. auris* strain we used displayed the aggregate-forming phenotype, which is a potential cause for its low virulence towards *G. mellonella*.

Given that antimicrobial treatment needs to be given at non-toxic doses to patients, it is essential that photodynamic treatments are not toxic to *G. mellonella* [27]. APDT with MB, NMBN, and TBO were ineffective in treating *G. mellonella* infected with *C. auris* or *C. albicans*. However, APDT with the novel pentacyclic phenothiazine S137 effectively treated *C. auris* and *C. albicans* infections in *G. mellonella*. The fact that only S137 managed to control *Candida* infection led us to hypothesize that its structural features give it advantages over the other PS. This hypothesis is further supported by the fact that S137 was active even in the absence of light, i.e., its greater effectiveness over the other phenothiazinium PS appears to be (at least partially) unrelated to its photochemical characteristics. Indeed, S137 is a much more lipophilic PS with a great affinity towards membrane lipids (Supplementary Figure 2) [48]. This increased affinity allows S137 to interact more strongly with cell membranes, causing disturbances that increase its permeability [18]. Also, a previous study has reported that S137 is effective against many species of *Candida* even in the dark [22]. Thus, the increased activity of S137 in our study is likely due to membrane disturbances that may, among other things, slow down fungal growth and make the pathogen more susceptible to the host's immune system.

Therefore, the *C. auris* strain used in this study displays multidrug-resistance to the antifungals commonly used in the clinic and is, as such, difficult to treat. Although APDT with MB, NMBN, TBO, and S137 have been effective against *C. auris in vitro*, only APDT with the new phenothiazinium PS S137 was effective in treating *C. auris*- or *C. albicans*-infected *G. mellonella*. Our results show that APDT with S137 is a promising therapy against *C. auris* infection and reinforce the importance of searching for new PS structures to improve APDT effectiveness against multidrug-resistant microorganisms.

Author Contributions: “Conceptualization, M.R.V.Z.K., G.U.L.B, M.W, and E.N; methodology, P.H.G.B, and L.T.; software, L.T.; validation, P.H.G.B, and L.T.; formal analysis, M.R.V.Z.K, P.H.G.B, and L.T.; investigation, M.R.V.Z.K, P.H.G.B., L.T., E.N., and G.T.P.B.; resources, M.R.V.Z.K.; data curation, M.R.V.Z.K; writing—original draft preparation, M.R.V.Z.K; writing—review and editing, P.H.G.B, L.T., E.N., G.U.L.B, G.T.P.B., and M.W; supervision M.R.V.Z.K; project administration, M.R.V.Z.K.; funding acquisition, M.R.V.Z.K. All authors have read and agreed to the published version of the manuscript.”

Funding: This research was funded by Fundação de Amparo à Pesquisa do Estado de São Paulo - Brazil (FAPESP), grant number 2017/25300-8 and 2020/07546-2. P.H.G.B., scholarship financed by the Coordenação de Aperfeiçoamento de Pessoal de Nível Superior – Brazil (CAPES) – Finance Code 001. G.T.P.B. would like to thank the National Council for Scientific and Technological Development for a post-doctoral fellowship (165191/2020-1).

Data Availability Statement: “Not applicable.”

Conflicts of Interest: “The authors declare no conflict of interest.”

References

1. Cortegiani, A.; Misseri, G.; Chowdhary, A. What’s new on emerging resistant *Candida* species. *Intensive Care Med.* **2019**, *45*, 512–515. doi:10.1007/s00134-018-5363-x
2. Chowdhary, A.; Sharma, C.; Meis, J.F. *Candida auris*: a rapidly emerging cause of hospital-acquired multidrug-resistant fungal infections globally. *PLoS Pathog.* **2017**, *13*, e1006290. doi: 10.1371/journal.ppat.1006290
3. Lockhart, S.R.; Etienne, K.A.; Vallabhaneni, S.; et al. Simultaneous emergence of multidrug-resistant *Candida auris* on 3 continents confirmed by whole-genome sequencing and epidemiological analyses. *Clin Infect Dis.* **2017**, *64*(2), 134–140. doi:10.1093/cid/ciw691
4. Ruiz-Gaitan, A.; Moret, A.M.; Tasiias-Pitarch, M.; et al. An outbreak due to *Candida auris* with prolonged colonisation and candidaemia in a tertiary care European hospital. *Mycoses* **2018**, *61*(7), 498–505. doi: 10.1111/myc.12781
5. Larkin, E.; Hager, C.; Chandra, J.; Mukherjee, P.K.; Retuerto, M.; Salem, I.; et al. The emerging pathogen *Candida auris*: growth phenotype, virulence factors, activity of antifungals, and effect of SCY-078, a novel glucan synthesis inhibitor, on growth morphology and biofilm formation. *Antimicrob. Agents Chemother.* **2017**, *61*(5), e02396-16. doi:10.1128/AAC.02396-16
6. Horton, M.V.; Johnson, C.J.; Kernien, J.F.; Patel, T.D.; Lam, B.C.; Cheong, J.Z.A.; et al. *Candida auris* forms high-burden biofilms in skin niche conditions and on porcine skin. *mSphere*, **2020**, *5*(1), e00910-19. doi:10.1128/mSphere.00910-19
7. Welsh, R.M.; Bentz, M.L.; Shams, A.; Houston, H.; Lyons, A.; Rose, L.J.; et al. Survival, persistence, and isolation of the emerging multidrug-resistant pathogenic yeast *Candida auris* on a plastic health care surface. *J Clin Microbiol.* **2017**, *55*(10), 2996–3005. doi:10.1128/JCM.00921-17
8. Du, H.; Bing, J.; Hu, T.; Ennis, C.L.; Nobile, C.J.; Huang, G. *Candida auris*: Epidemiology, biology, antifungal resistance, and virulence. *PLoS Pathog* **2020**, *16*(10), e1008921. doi:10.1371/journal.ppat.1008921
9. Hata, D.J.; Humphries, R.; Lockhart, S.R. College of American Pathologists Microbiology Committee. *Candida auris*: an emerging yeast pathogen posing distinct challenges for laboratory diagnostics,

- treatment, and infection prevention. *Arch Pathol Lab Med.* **2020**; *144*(1),107–114. doi:10.5858/arpa.2018-0508-RA
10. Chowdhary, A.; Prakash, A.; Sharma, C.; Kordalewska, M.; Kumar, A.; Sarma, S.; et al. A multicentre study of antifungal susceptibility patterns among 350 *Candida auris* isolates (2009-17) in India: role of the ERG11 and FKS1 genes in azole and echinocandin resistance. *J Antimicrob Chemother.* **2018**, *73*, 891–899. Doi: 10.1093/jac/dkx480
11. Sabino, P.S.; Wainwright, M.; Ribeiro, M.S.; Sellera, F.P.; Anjos, C.; Baptista, M.S.; Lincopan, N. Global priority multidrug-resistant pathogens do not resist photodynamic therapy. *J. Photochem. Photobiol. B, Biol.* **2020**, *208*, 111893. doi:10.1016/j.jphotobiol.2020.111893.
12. Bapat, P.S.; Nobile, C.J. Photodynamic therapy is effective against *Candida auris* biofilms. *Front. Cell. Infect. Microbiol.* **2021**, *11*, 713092. doi:10.3389/fcimb.2021.713092
13. Hamblin, M.; Hassan T. Photodynamic therapy: a new antimicrobial approach to infectious disease? *Photochem Photobiol Sci* **2004**, *3*, 436–450. doi:10.1039/b311900a
14. Wainwright, M.; Crossley, K.B. Methylene Blue – a therapeutic dye for all seasons? *J. Chemother.* **2002**, *14*, 431–443. doi: 10.1179/joc.2002.14.5.431
15. Tseng, S.P.; Hung, W.C.; Chen, H.J.; Lin, Y.T.; Jiang, H.S.; Chiu, H.C.; Hsueh, P.R.; Teng, L.J.; Tsai, J.C. Effects of toluidine blue O (TBO)-photodynamic inactivation on community-associated methicillin-resistant *Staphylococcus aureus* isolates. *J. Microbiol. Immunol. Infect.* **2015**, *50*(1), 46-54. doi: 10.1016/j.jmii.2014.12.007
16. Andrade, G.C; Brancini, G.T.P.; Abe, F.R.; Oliveira, D.P.; Nicoletta, H.D.; Tavares, D.C.; Micas, A.F.D.; Savazzi, E.A.; Silva-Junior, G.J.; Wainwright, M.; Braga, G.U.L. Phenothiazinium dyes for photodynamic treatment present lower environmental risk compared to a formulation of trifloxystrobin and tebuconazole. *J. Photochem. Photobiol. B, Biol.* **2022**, *226*, 112365, doi: 10.1016/j.jphotobiol.2021.112365
17. Abrahamse, H.; Hamblin, M.R. New photosensitizers for photodynamic therapy. *Biochem. J.* **2016**, *473*, 347–364. doi: 10.1042/BJ20150942
18. Rodrigues, G.B.; Brancini, G.T.P.; Uyemura, S.A.; Bachmann, L.; Wainwright, M.; Braga, G.U.L. Chemical features of the photosensitizers new methylene blue N and S137 influence their subcellular localization and photoinactivation efficiency in *Candida albicans*. *J. Photochem. Photobiol. B, Biol.* **2020**, *209*, 111942. doi: 10.1016/j.jphotobiol.2020.111942
19. Wainwright, M.; Meegan, K.; Loughran, C.; Giddens, R.M. Phenothiazinium photosensitisers VI. Photobactericidal asymmetric derivatives. *Dyes Pigm.* **2009**, *82*, 387–391. doi: 10.1016/j.dyepig.2009.02.011
20. Wainwright, M.; Meegan, K.; Loughran, C. Phenothiazine photosensitisers IX. Tetra- and pentacyclic derivatives as photoantimicrobial agents. *Dyes Pigm.* **2011**, *91*, 1–5. doi:10.1016/j.dyepig.2011.02.001

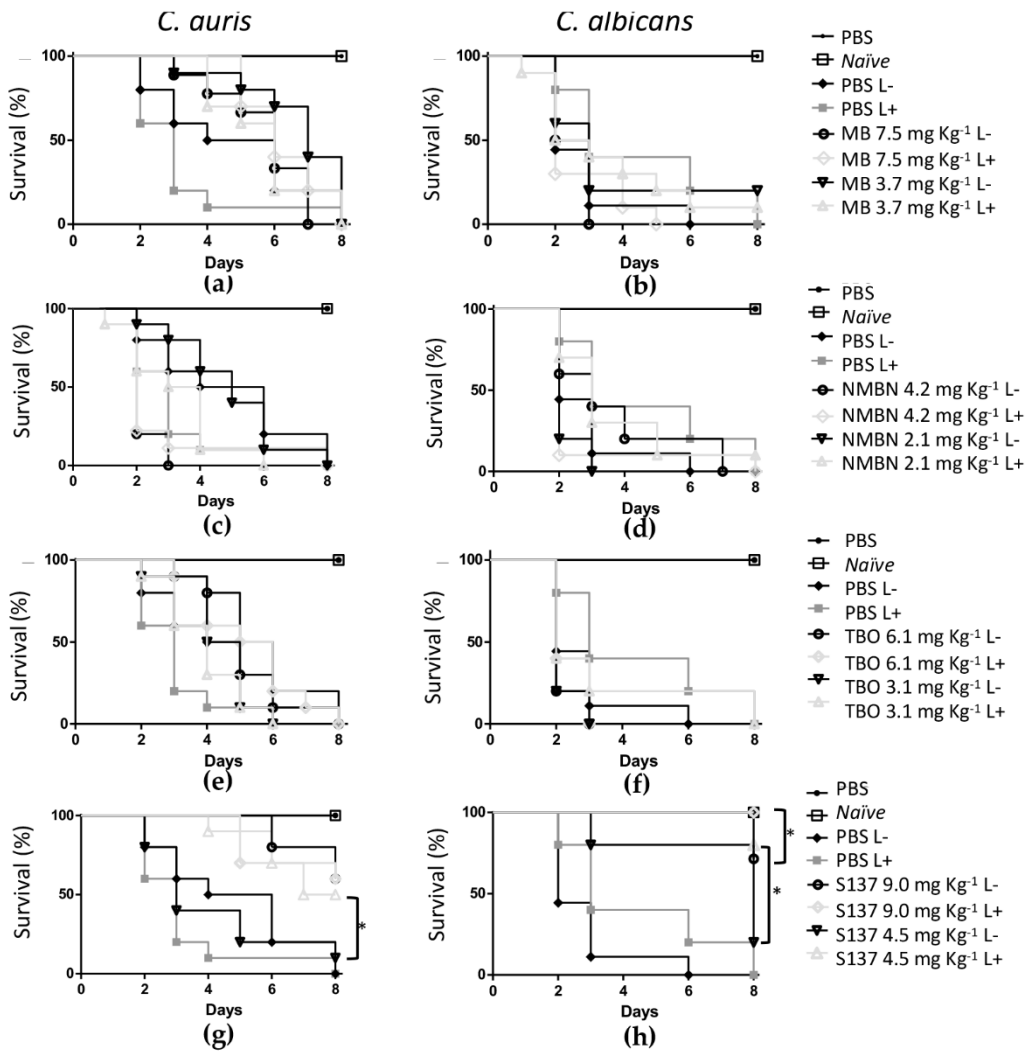
-
21. Teichert, M.C.; Jones, J.W.; Usacheva, M.N.; Biel, M.A. Treatment of oral candidiasis with methylene blue-mediated photodynamic therapy in immunodeficient murine model. *Oral Surg. Oral Med. Oral Pathol. Oral Radiol. Endod.* **2002**, *93*, 155–160. doi: 10.1067/moe.2002.120051
22. Rodrigues, G.B.; Dias-Baruffi, M.; Holman, N.; Wainwright, M.; Braga, G.U.L. In vitro photodynamic inactivation of *Candida* species and mouse fibroblasts with phenothiazinium photosensitizers and red light. *Photodiagn. Photodyn. Ther.* **2013**, *10*, 141e149. doi: 10.1016/j.pdpdt.2012.11.004
23. Tan, J.; Liu, Z.; Sun, Y.; et al. Inhibitory effects of photodynamic inactivation on planktonic cells and biofilms of *Candida auris*. *Mycopathologia* **2019**, *184*, 525–531. doi: 10.1007/s11046-019-00352-9
24. Bapat, P.; Singh, G.; Nobile, C.J. Visible lights combined with photosensitizing compounds are effective against *Candida albicans* biofilms. *Microorganisms* **2021**, *9*, 500. doi: 10.3390/microorganisms9030500
25. Gonzales, F.P.; da Silva, S.H.; Roberts, D.W.; Braga, G.U.L. Photodynamic inactivation of conidia of the fungi *Metarhizium anisopliae* and *Aspergillus nidulans* with methylene blue and toluidine blue. *Photochem. Photobiol.* **2010**, *86*, 653–661. doi: 10.1111/j.1751-1097.2009.00689.x
26. de Menezes, H.D.; Tonani, L.; Bachmann, L.; Wainwright, M.; Braga, G.U.L.; von Zeska Kress, M.R. Photodynamic treatment with phenothiazinium photosensitizers kills both ungerminated and germinated microconidia of the pathogenic fungi *Fusarium oxysporum*, *Fusarium moniliforme* and *Fusarium solani*. *J. Photochem. Photobiol. B Biol.* **2016**, *164*, 1–12. doi: 10.1016/j.jphotobiol.2016.09.008.
27. Paziani, M.H.; Tonani, L.; de Menezes, H.D.; Bachmann, L.; Wainwright, M.; Braga, G.U.L.; von Zeska Kress, M.R. Antimicrobial photodynamic therapy with phenothiazinium photosensitizers in non-vertebrate model *Galleria mellonella* infected with *Fusarium keratoplasticum* and *Fusarium moniliforme*. *Photodiagnosis Photodyn Ther.* **2019**, *25*, 197–203. doi: 10.1016/j.pdpdt.2018.12.010
28. de Menezes, H.D.; Rodrigues, G.B.; Teixeira, S.D.P.; Massola, N.S.; Bachmann, L.; Wainwright, M.; Braga, G.U.L. In vitro photodynamic inactivation of plant-pathogenic fungi *Colletotrichum acutatum* and *Colletotrichum gloeosporioides* with novel phenothiazinium photosensitizers. *Appl. Environ. Microbiol.* **2014**, *80*(5), 1623–1632. doi:10.1128/AEM.02788-13
29. Fracarolli, L.; Rodrigues, G.B.; Pereira, A.C.; Massola Júnior, N.S.; Silva-Junior, G.J.; Bachmann, L.; Wainwright, M.; Bastos, J.K.; Braga, G.U.L. Inactivation of plant-pathogenic fungus *Colletotrichum acutatum* with natural plant-produced photosensitizers under solar radiation. *J. Photochem. Photobiol. B Biol.* **2016**, *162*, 402–411. doi: 10.1016/j.jphotobiol.2016.07.009
30. Gonzales, J.C.; Brancini, G.T.P.; Rodrigues, G.B.; Silva-Junior, G.J.; Bachmann, L.; Wainwright, M.; Braga, G.U.L. Photodynamic inactivation of conidia of the fungus *Colletotrichum abscissum* on *Citrus sinensis* plants with methylene blue under solar radiation. *J. Photochem. Photobiol. B Biol.* **2017**, *176*, 54–61. doi: 10.1016/j.jphotobiol.2017.09.008

-
31. Tonani, L.; Morosini, N.S.; de Menezes, H.D.; Bonifácio da Silva, M.E.N.; Wainwright, M.; Braga, G.U.L.; von Zeska Kress, M.R. In vitro susceptibilities of *Neoscytalidium* spp. sequence types to antifungal agents and antimicrobial photodynamic treatment with phenothiazinium photosensitizers. *Fungal Biol.* **2018**, *122*(6), 436-448. doi: 10.1016/j.funbio.2017.08.009
32. Lu, Q.; Sun, Y.; Tian, D. et al. Effects of Photodynamic Therapy on the Growth and Antifungal Susceptibility of *Scedosporium* and *Lomentospora* spp. *Mycopathologia* **2017** *182*, 1037–1043. doi: 10.1007/s11046-017-0195-8
33. Gao, L.; Jiang, S.; Sun, Y.; Deng, M.; Wu, Q.; Li, M.; Zeng, T. Evaluation of the Effects of Photodynamic Therapy Alone and Combined with Standard Antifungal Therapy on Planktonic Cells and Biofilms of *Fusarium* spp. and *Exophiala* spp. *Front Microbiol.* **2016** Apr 27;7:617. doi: 10.3389/fmicb.2016.00617
34. Liu Z, Tang J, Sun Y, Gao L. Effects of Photodynamic Inactivation on the Growth and Antifungal Susceptibility of *Rhizopus oryzae*. *Mycopathologia.* **2019** Apr;184(2):315-319. doi: 10.1007/s11046-019-00321-2
35. Fakhim, H.; Vaezi, A.; Dannaoui, E.; Chowdhary, A.; Nasiry, D.; Faeli, L.; Meis, J.F.; Badali H. Comparative virulence of *Candida auris* with *Candida haemulonii*, *Candida glabrata* and *Candida albicans* in a murine model. *Mycoses* **2018**, *61*(6), 377-382 doi: 10.1111/myc.12754
36. Borman, A.M.; Szekely, A.; Johnson, E.M. Comparative pathogenicity of United Kingdom isolates of the emerging pathogen *Candida auris* and other key pathogenic *Candida* species. *mSphere* **2016**, *1*(4). doi: 10.1128/mSphere
37. Romera, D.; Aguilera-Correa, J.J.; García-Coca, M.; Mahillo-Fernández, I.; Viñuela-Sandoval, L.; García-Rodríguez, J.; Esteban, J. The *Galleria mellonella* infection model as a system to investigate the virulence of *Candida auris* strains. *Pathog. Dis.* , *78*(9), ftaa067. doi: 10.1093/femspd/ftaa067
38. Ames, L.; Duxbury, S.; Pawlowska, B.; Ho, H.; Haynes, K.; Bates, S. *Galleria mellonella* as a host model to study *Candida glabrata* virulence and antifungal efficacy. *Virulence* **2017**, *8*(8), 1909-1917. doi: 10.1080/21505594.2017.1347744
39. Figueiredo-Godoi, L.M.A.; Menezes, R.T.; Carvalho, J.S.; Garcia, M.T.; Segundo, A.G.; Jorge, A.O.C.; Junqueira, J.C. Exploring the *Galleria mellonella* model to study antifungal photodynamic therapy. *Photodiagnosis Photodyn. Ther.* **2019**, *27*, 66-73. doi: 10.1016/j.pdpdt.2019.05.010
40. Clinical and Laboratory Standards Institute, Reference Method for Broth Dilution Antifungal Susceptibility Testing of Yeasts, 3rd ed., Clinical and Laboratory Standards Institute, Wayne, PA, **2008** Approved standard M27-A3. ISBN 1-56238-666-2 ISSN 0273-3099
41. Pierce, C.G.; Uppuluri, P.; Tristan, A.R; Wormley Jr, F.L.; Mowat, E.; Ramage, G.; Lopez-Ribot, J.L. A simple and reproducible 96-well plate-based method for the formation of fungal biofilms and its application to antifungal susceptibility testing. *Nat. Protoc.* **2008**, *3*(9), 1494-1500. doi: 10.1038/nprot.2008.141

-
42. Li, X.; Gao, M.; Han, X.; Tao, S.; Zheng, D.; Cheng, Y.; Yu, R.; Han, G.; Schmidt, M.; Han, L. Disruption of the phospholipase D gene attenuates the virulence of *Aspergillus fumigatus*. *Infection and Immunity*. **2012**, *1*(80), 429-440. doi: 10.1128/IAI.05830-11
43. Seidler, M.J.; Salvenmoser, S.; Müller, F.M. *Aspergillus fumigatus* forms biofilms with reduced antifungal drug susceptibility on bronchial epithelial cells. *Antimicrob. Agents Chemother.* **2008**, *52*(11), 4130-4136. doi: 10.1128/AAC.00234-08
44. Horton, M.V.; Nett, J.E. *Candida auris* infection and biofilm formation: going beyond the surface. *Curr. Clin. Microbiol. Rep.* **2020**, *7*(3), 51-56. doi: 10.1007/s40588-020-00143-7
45. Thompson, D.S.; Carlisle, P.L.; Kadosh, D. Coevolution of morphology and virulence in *Candida* species. *Eukaryot. Cell*. **2011**, *10*(9), :1173-1182. doi: 10.1128/EC.05085-11
46. Yue, H.; Bing, J.; Zheng, Q.; Zhang, Y.; Hu, T.; Du, H.; et al. Filamentation in *Candida auris*, an emerging fungal pathogen of humans: passage through the mammalian body induces a heritable phenotypic switch. *Emerg. Microbes Infect.* **2018**, *7*(1), 188. doi: 10.1038/s41426-018-0187-x PMID: 30482894
47. Brown, J.L.; Delaney, C.; Short, B.; Butcher, M.C.; McKlound, E.; Williams, C.; Kean, R.; Ramage, G. *Candida auris* phenotypic heterogeneity determines pathogenicity in vitro. *mSphere* **2020**, *5*, e00371-20. doi: 10.1128/mSphere.00371-20
48. Bacellar, I.O.L.; Oliveira, M.C.; Dantas, L.S.; Costa, E.B.; Junqueira, H.C.; Martins, W.K.; Durantini, A.M.; Cosa, G.; Di Mascio, P.; Wainwright, M.; Miotto, R.; Cordeiro, R.M.; Miyamoto, S.; Baptista, M.S. Photosensitized Membrane Permeabilization Requires Contact-Dependent Reactions between Photosensitizer and Lipids. *J. Am. Chem. Soc.* **2018**, *140*(30), 9606-9615 doi: 10.1021/jacs.8b05014

Supplementary figures:

Supplementary figure 01:



543

544

545

546

547

548

549

550

551

552

553

554

555

556

557

558

559

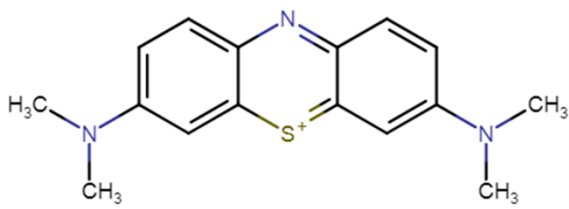
560

561

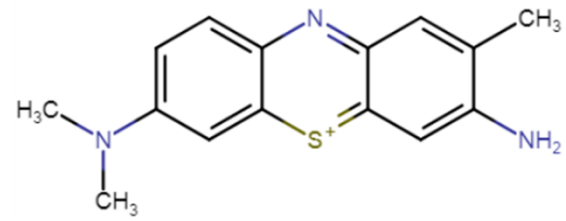
Supplementary figure 02:

562

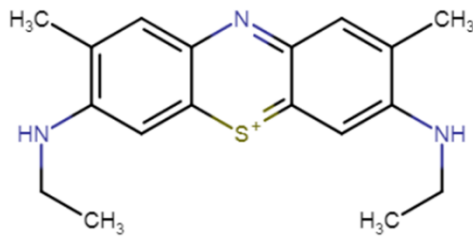
563



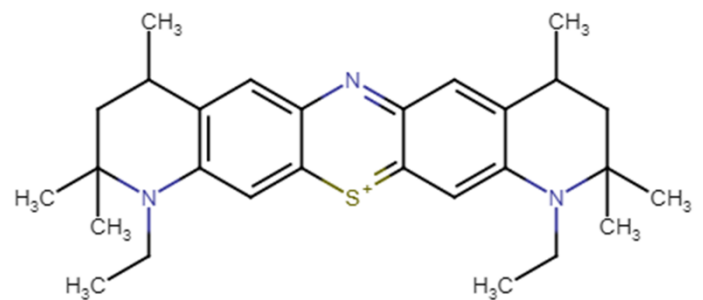
Methylene blue
 $\log P = 2.61$



Toluidine blue
 $\log P = 2.19$



New methylene blue N
 $\log P = 3.08$



S137
 $\log P = 6.26$

564